

Ion Transport in Micelle-like Films: Soft-Landed Ion Studies

Kai Wu, Martin J. Iedema, and James P. Cowin*

Pacific Northwest National Laboratory, Box 999, M/S K8-88, Richland, Washington 99352

Received June 30, 1999. In Final Form: January 24, 2000

Ion-transport processes across epitaxially grown micelle-like films in the form of liquid hydrocarbon/water/hydrocarbon sandwiches were studied by a novel ion soft-landing technique. Centered inside of vapor-deposited glassy films of 3-methylpentane (166 monolayers) and methylcyclohexane (50 monolayers) was a water layer from 0 to 10 monolayers thick. From 90 to 150 K we time-resolved hydronium ion motion and found that the ions (D_3O^+) clearly paused in the aqueous phase, being transiently trapped by solvation interactions. A modified Born solvation model qualitatively showed that a trap energy gradually built up in the aqueous phase with the water layer thickness.

Introduction

Micelles play important roles in areas as diverse as drug carriers, detergents, organic synthesis, froth flotation, and petroleum recovery.¹ Many applications involve the transport of substances across the aqueous/organic interfaces in the micelles. Immiscible aqueous/organic interfaces can also profoundly affect ion transport, which is common in biology, electrochemistry, and even nuclear waste treatments.^{2–5} Here we report a study that shows how the aqueous phase in vapor-deposited, micelle-like films affects ion transport.

Our micelles are really planar models based on ultrathin films. They have the structure of organic/aqueous/organic, so are perhaps more akin to “reverse micelles” that are formed from aqueous additions to organic solvents.¹ Their geometry is very well-defined, as they are vapor-deposited onto a cryogenic substrate with a molecular beam, with molecular monolayer precision. Inside of the organic film is placed 0 to 10 monolayers of water, to act as a solvation trap for ions. The studies are done above the glass temperature of the organics, where they become true liquids. Much of the ion motion occurs before the neutral water can diffuse, so the geometry of the films is uniquely well-determined.

We use a very-low-energy ion beam to place pure ions (hydronium) directly upon one side of the micelle-like films, in a vacuum. The other side of the micelle is against a planar Pt single-crystal disk. The ions produce a net voltage across the film, which depends on their position. We measure this voltage to monitor the ion motion. The film acts as a planar capacitor. Ion deposition is essentially a charging process of the capacitor. The capacitance of the planar capacitor can be expressed as $C = Q/V$, where V is the potential difference across the capacitor and Q is the total charge on either plate of the capacitor. It can also be expressed as $C = \epsilon_0 \epsilon A/L$, where L is the distance

between the plates of the capacitor, ϵ_0 is the vacuum permittivity, ϵ is the permittivity (dielectric constant) of the medium in the capacitor, and A is the area of either plate. Combining the two equations, we obtain $V = QL/\epsilon_0 \epsilon A$.

When the ions move in the film, they create a charge distribution $\rho(z)$ (z is the axis perpendicular to the film surface; any x or y dependence does not contribute to the film voltage change). One can easily show that any narrow charge distribution on top of the film quickly turns into a square distribution along z under the influence of the ion self-generated electric field. The ions in the front experience the highest field, move the fastest, and hence stay in front. For a uniform film, if we denote the average height of the ions above the substrate surface (the bottom of the film) as h , then the film voltage can be shown to be⁶

$$V = \frac{1}{\epsilon \epsilon_0} \int_0^L dz \rho(z) z = \frac{Qh}{\epsilon \epsilon_0 A} \quad (1)$$

Under our conditions no ion neutralization occurs, so Q is constant, as are ϵ_0 and A . Since ϵ for hydrocarbons is also nearly constant,⁷ any change in V directly monitors the ion motion in the bulk film through h . V is measured with a noncontacting Kelvin probe. For our micelle system there is a water layer in the middle of the organic film. Since it has a much higher dielectric constant than the hydrocarbon and is thin compared to the hydrocarbon, the water layer acts like a large capacitance in series with the smaller values for the hydrocarbon layers. The Kelvin probe voltage is thus insensitive to the water layer's presence: it basically “shorts” the hydrocarbon films together. For a micelle, the integral in eq 1 is valid to a good approximation if one integrates only over the hydrocarbon regions, subtracting the water film thickness from z when z is above the water layer and attributing all ions within the water layer to be in a delta function at the top of the lower hydrocarbon film. The effect of the water film is not negligible, though it can (and does) profoundly alter the time evolution of the $\rho(z)$ distribution.

In this report, two case studies will be shown for hydronium ion migration: across the methylcyclohexane

(1) Jones, M. N.; Chapman, D., III; Jones, M. *Micelles, Monolayers, and Biomembranes*; John Wiley & Sons: New York, 1994.

(2) Starks, C. M.; Liotta, C. L.; Halpern, M. *Phase-transfer Catalysis—Fundamentals, Applications and Industrial Perspectives*; Chapman & Hall: New York, 1994.

(3) Edzes, H. T.; Berendsen, H. J. C. *Annu. Rev. Biophys. Biophys. Chem.* **1975**, *5*, 265.

(4) Sen, R. K.; Yeager, E.; O'Grady, W. E. *Annu. Rev. Phys. Chem.* **1975**, *26*, 287.

(5) Noyes, R. *Nuclear Waste Cleanup Technology and Opportunities*; Noyes Publication: Park Ridge, 1995.

(6) Tsekouras, A. A.; Iedema, M. J.; Cowin, J. P. *J. Chem. Phys.* **1999**, *111*, 2222.

(7) *Handbook of Chemistry and Physics*; Lide, D. R., Ed.; CRC: Boca Raton, FL, 1995.

(MCH)/H₂O/MCH and 3-methylpentane (3MP)/H₂O/3MP sandwich films. Then the energetics of the system will be analyzed by a modified Born solvation model to explain our experimental observations.

Experimental Section

Details of the experimental technique have been described elsewhere.^{8,9} The system consists of three main components: a main ultrahigh vacuum (UHV) chamber, an ion source, and a three-stage differentially pumped molecular beam.

All experimental measurements were carried out in the main UHV chamber with a base pressure of 2×10^{-10} Torr. The chamber has a McAllister Kelvin probe¹⁰ for monitoring the film voltage change, a quadrupole mass spectrometer (UTI) for measuring temperature-programmed desorption (TPD) spectra, a sputtering ion gun for cleaning the sample, and an Auger electron spectrometer for monitoring surface cleanliness. A Pt(111) disk (10 mm in diameter) was used as the substrate to grow the organic films and was atomically cleaned by conventional methods. The sample was cooled to 30 K with a closed cycle He refrigerator and could be heated radiatively on its back by four W filaments at linear ramping rates varying from several degrees per second to tenths of a degree per second in the temperature range 30 to 1200 K. Two K-type thermocouples were welded at the sample sides to measure the temperature and to bias or ground the sample.

The molecular beam was used to vapor deposit sandwiches of MCH or 3MP and water at 30 K. Their coverages were calibrated by using TPD to determine the dose to achieve a saturated first monolayer (ML), following the methods reported in the literature.^{11,12} MCH and 3MP are true liquids above their glass temperatures T_g of 85 and 77 K, respectively. Above T_g their viscosity rapidly decreases with increasing temperature.^{13,14}

The ion source produced pure, mass-selected hydronium ions (D₃O⁺). The D₃O⁺ ion beam⁸ had a current of 1–3 nA and a beam diameter of about 0.9 cm (0.64 cm² in area). Ions were gently landed on the film surface at 30 K at a kinetic energy of <1.2 eV. This required continuous changing of the sample bias voltage as the film was charged up. The ion current during the ion deposition was integrated to yield Q .

It was crucial to suppress water contamination from both the ion source and the main UHV chamber background. To do this, the ion path was bent 5° twice, and two liquid nitrogen traps were used. TPD measurements showed that the unintended water contamination from both D₂O and H₂O was <0.01 ML.

After deposition of typically 0.0001–0.01 ML of ions, the sample was warmed at 0.2 K/s, during which the film voltage was measured by the Kelvin probe and desorption of the organic film was monitored by the mass spectrometer ($m/z = 83, 57, \text{ and } 18$ for MCH, 3MP, and H₂O, respectively). Prior to use, the high-purity MCH, 3MP, and H₂O were further degassed by freeze–pump–thaw treatments. Stray electron effects were eliminated by turning the mass spectrometer off until the ions had moved through the organic films and turning it on before the film desorption commenced. The secondary electrons from the double-mesh ion decelerator were eliminated by an 80 G magnet field.⁸

Results and Discussion

1. Ion Motion Delayed by Added Water. Figure 1 shows the temperature evolution of the film voltage (trace b) for D₃O⁺ motion in the micelle-like sandwich: 83 ML 3MP/2 ML H₂O/83 ML 3MP (about 60 nm in total

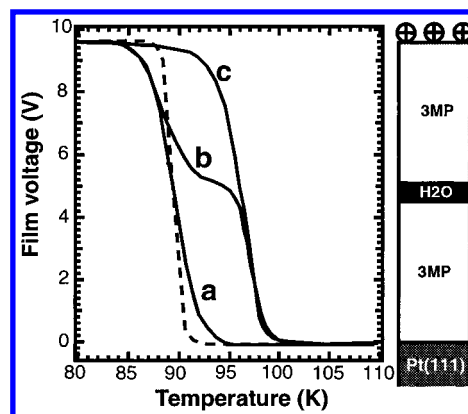


Figure 1. Temperature evolution of the film voltage for D₃O⁺ migration through (a) the pure 166 ML 3MP film, (b) the micelle-like 83 ML 3MP/2 ML H₂O/83 ML 3MP sandwich film, and (c) the 2 ML H₂O/166 ML 3MP film. The broken curve is theoretically calculated for ion motion in 166 ML 3MP, on the basis of the ion drift model.⁶ All films were grown at 30 K, and the temperature was ramped at 0.2 K/s. The simple drawing on the right side of the figure shows the film structure, not in proportion.

thickness), all deposited at 30 K. Initially the ions create a film voltage of 9.6 V. The film voltage does not change below 80 K. When temperature is further ramped, the voltage rapidly decreases between 84 and 92 K (with a maximum-slope temperature at 87 K). The voltage hesitates between 92 and 98 K and then rapidly drops between 98 and 100 K. While there are many important features, the most striking is that the pause in voltage near 95 K is at about half of the initial voltage, just what would be expected from eq 1 if the ions migrate down and become temporarily trapped in the thin aqueous layer. Because an ion of charge q_i , when placed in the field generated by a voltage V across the film, moves faster than a neutral (discussed later),⁶ the water layer is *not* expected to be able to diffuse before being sampled by the ions.

Also shown in Figure 1 is the temperature evolution of the film voltage for D₃O⁺ in pure 166 ML 3MP (trace a), that is, the above-described sandwich film with the water layer left out. Without the water layer in the middle of the film, the voltage just drops in a single step between 84 and 94 K with no pause. This clearly indicates that the pause in voltage for the sandwich film is due to the water layer. We also studied the D₃O⁺ motion in 2 ML H₂O/166 ML 3MP films, at similar fields to that for the original sandwich film, as displayed by trace c in Figure 1. It is very similar to the second drop of the V versus T curve (trace 1b) for the micelle-like film. Trace 1c does not show the first voltage drop as for the micelle-like film because the water layer of the 2 ML H₂O/166 ML 3MP film immediately traps the ions before they can migrate. The latter two experiments imply that D₃O⁺ motion in the sandwich film can be decomposed into two independent kinetic steps: migration in pure 3MP and traversing/escaping the H₂O layer.

Hydronium ion motion in the pure hydrocarbons can be independently estimated. If the ions move with a drift velocity proportional to the applied field and in inverse proportion to the 3MP viscosity and ion hydrodynamic radius, as in the Stokes–Einstein equation, the motion of the ions in pure 3MP should be estimable from the known viscosity data.¹³ Using numerical integration of the ion migration equations,⁶ one can predict the temperature evolution of the film voltage for D₃O⁺ in pure 3MP. This is shown by the broken curve in Figure 1 with

(8) Biesecker, J. P.; Ellison, G. B.; Wang, J.; Iedema, M. J.; Tsekouras, A. A.; Cowin, J. P. *Rev. Sci. Instrum.* **1998**, *69*, 485.

(9) Tsekouras, A. A.; Iedema, M. J.; Ellison, G. B.; Cowin, J. P. *Int. J. Mass Spectrom. Ion Processes* **1998**, *174*, 219.

(10) McAllister Technical Services, Coer d'Alene, Idaho, Model KP6500.

(11) Materer, N.; Starke, U.; Barbieri, A.; van Hove, M. A.; Somorjai, G. A.; Kroes, G. J.; Monot, C. *Surf. Sci.* **1997**, *381*, 190.

(12) Jiang, L. Q.; Avoyan, A.; Koel, B. E.; Falconer, J. L. *J. Am. Chem. Soc.* **1993**, *115*, 12106.

(13) Ling, A. C.; Willard, J. E. *J. Phys. Chem.* **1968**, *72*, 1918.

(14) Carpenter, M. R.; Davies, D. B.; Matheson, A. J. *J. Chem. Phys.* **1967**, *46*, 2452.

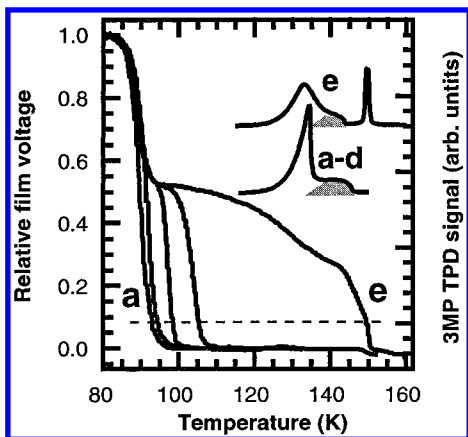


Figure 2. Rescaled temperature evolution of the film voltage as a function of the thickness of the added water layer in the 83 ML 3MP/H₂O/83 ML 3MP sandwich film. The water coverage is (a) 0.0, (b) 1.0, (c) 2.0, (d) 4.0, and (e) 10 ML (the unscaled starting voltages were 7.6, 8.5, 9.7, 9.6, and 8.9 V, respectively). Also shown are the corresponding TPD profiles of 3MP. The sharp peak at about 150 K of the TPD profile (e) is due to the volcanic desorption of 3MP.¹⁵ The “split” feature of the TPD profiles (the shaded areas) is due to the Kelvin probe. About half of the surface area is blocked by the probe, so that the desorbing molecules behind the probe are forced to bounce between the substrate surface and the Kelvin probe for many times before they completely escape and thus have to desorb from the film multiple times. Refer to ref 6 for more details. The dashed line intersects the curves at the temperatures that are to be plotted in Figure 5.

a film thickness of 166 ML and an ion radius of 3 Å. Note that the square distribution of the ions is already included in the simulation. The theoretical calculation is in fair agreement with the experimental result, giving the correct maximum-slope temperature of the film voltage change.

2. Effect of the Added Water Layer Thickness.

Figure 2 shows the effect of the thickness of the added water layer on the ion transport in the micelles. For the sake of convenience in comparison of the V versus T curve shapes, all initial voltages (≈ 8 – 10 V) have been rescaled to 1. It is clear that, with the increase of the water layer thickness, the voltage pause becomes more and more remarkable and the second voltage drop shifts to higher temperatures. For the 10 ML H₂O case, the film voltage stays at half of the initial value over a very broad temperature range (95–120 K) until 3MP desorption starts. The 10 ML water layer essentially forms an impermeable barrier to ion motion. This film also partially blocks the evaporation of the underlying 3MP molecules. This creates the so-called “molecular volcano” eruption when cracks are abruptly formed during water–ice crystallization,¹⁵ as shown in Figure 2 by the very narrow TPD peak of 3MP around 150 K, much higher than the normal 3MP desorption temperature, 134 K. In all curves for water coverage > 1 ML in Figure 2, the film voltage clearly lingers at half of the initial voltage, unambiguously showing that the ions are trapped by the aqueous phase.

3. Probing the Aqueous Phase Position.

In our experiments, motion of neutral molecules (either 3MP or water) is expected to be much slower than that of the ions. The time ratio for a monovalent ion to traverse a certain distance in the film via field-assisted drift versus via random diffusion can approximately be expressed as Vq/kT .⁶ For $V = 5$ V, the ion mobility is about 580 times more effective than the ions’ random diffusion at 100 K. Random

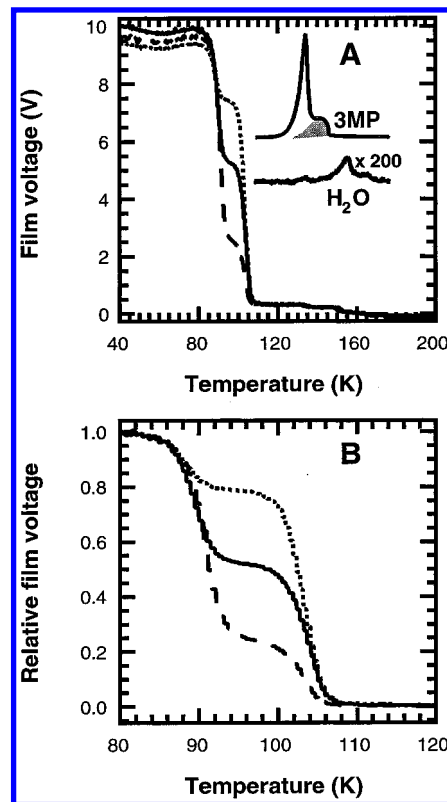


Figure 3. (A) Temperature evolution of the film voltage for 41 ML 3MP/4ML H₂O/125 ML 3MP (dotted curve), 83 ML 3MP/4ML H₂O/83 ML 3MP (solid curve), and 125 ML 3MP/4ML H₂O/41 ML 3MP. Also shown are the TPD profiles for 3MP ($\times 1$) and H₂O ($\times 200$). Again the shaded area in the TPD profile is due to the blocking effect of the Kelvin probe. (B) Corresponding temperature evolution curves of the rescaled film voltage.

diffusion of neutrals is expected to be similar to that for ions, to the extent that the Stokes law for random diffusion holds ($D = kT/(6\pi r_0 \eta)$, where r_0 is the ion hydrodynamic radius and η is the solvent viscosity) and the neutral and ion have similar sizes. Therefore, the aqueous phase should be able to be sensed by the probing ions before the water molecules diffuse into the 3MP films. If we bury the water layer in different positions of the 3MP film, the ions should pause at different positions and the film voltage profile should reflect the difference. Figure 3 displays the results. When the water layer is inserted at $1/4$, $1/2$, and $3/4$ of the 3MP film height (166 ML), the voltage pause occurs expectedly at about $1/4$, $1/2$, and $3/4$ of the initial film voltage, respectively, which can be clearly seen by the rescaled film voltage curves in Figure 3B. This further demonstrates that the voltage pause at half of the initial voltage in Figures 1 and 2 is due to the trapping of the ions by the aqueous phase. Simultaneous voltage and TPD measurements are shown in Figure 3 A, demonstrating that ions have already moved through the films far below the temperatures where either 3MP or water desorbs, provided that the water layer is thin enough (4 ML in Figure 3).

4. More Evidence for the Ion Motion Retardation.

The sudden hesitation of the ion motion in the micelle-like sandwich film is observed not only for 3MP/H₂O/3MP but also for MCH/H₂O/MCH. This is shown in Figure 4 with 4ML H₂O in both 3MP (dotted curve) and MCH (solid curve). The appearance of the voltage pause between 100 and 108 K for the 25 ML MCH/4 ML H₂O/25 ML MCH sandwich again shows that the ions are temporarily trapped by the water phase. However, the temperature evolution of the film voltage for the MCH/H₂O/MCH

(15) Smith, R. S.; Huang C.; Wong E. K. L.; Kay B. D. *Phys. Rev. Lett.* **1997**, *79*, 909.

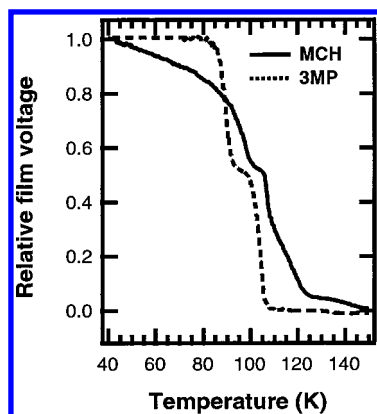


Figure 4. Temperature evolution of the film voltage for 25 ML MCH/4 ML H₂O/25 ML MCH (broken line) and 83 ML 3MP/4 ML H₂O/83 ML (solid line) sandwiches. The initial voltages are rescaled to 1.0 so that their shapes can be compared. Their electric fields are about 1×10^9 and 2×10^8 V/m. The ferroelectricity of the films¹⁶ and the work function changes due to their first chemisorbed monolayer are subtracted before the rescaling.

sandwich also shows some extra features that are not present for 3MP/H₂O/3MP. First, ions are already moving well below 85 K (the glass temperature for MCH¹³). Second, the voltage does not immediately go to zero above 120 K after they move past the water layer. And third, the pause in the film voltage happens between 100 and 106 K, about 8 K higher than that for 3MP/H₂O/3MP.

A theoretical prediction based on the simple viscosity model (not shown here) shows that the ions should not move in pure MCH below 85 K. This discrepancy is associated with “high”-electric-field effects on ion motion. In our extensive studies of hydronium ion motion in pure MCH,¹⁷ we have shown that, under fields at or above 0.01 V/Å (1×10^8 V/m), severe deviations from the Stokes–Einstein equation occur. In the present case for MCH, the field is at 0.1 V/Å (10^9 V/m). For 3MP here the electric field is less: 0.02 V/Å (2×10^8 V/m). The higher temperature for reaching the trap in MCH is easily attributable to its higher glass temperature and its relatively higher viscosity compared to that of 3MP at the same temperature. The starting temperatures for the ion motion delay in 3MP/H₂O/3MP and MCH/H₂O/MCH are 92 and 100 K, at which the published viscosities of 3MP and MCH are similar: 1.4×10^4 and 4.6×10^4 kg m⁻¹ s⁻¹.^{13,14,17} The reason for the higher temperature at which ions escape the trap for MCH is not immediately obvious and is discussed later.

The surprising tail in the voltage versus temperature for MCH after the ions escape the aqueous layer above 110 K is attributed to the partial crystallization of MCH on the Pt(111) substrate. Our detailed investigation¹⁷ shows that MCH tends to crystallize on Pt(111) above 110 K, giving tails in the voltage versus temperature curves. When the MCH film is preannealed to 139 K, the ions hardly move until 137 K.¹⁷ In this experiment the MCH film only partially crystallizes. In contrast to MCH, 3MP never crystallizes on the Pt(111) substrate, so no tail can be observed in the V versus T curves for 3MP (see the voltage curves in Figures 1–3).

5. Energetics Analysis. The temperature at which ions escape the 83 ML 3MP/water/83 ML 3MP sandwich

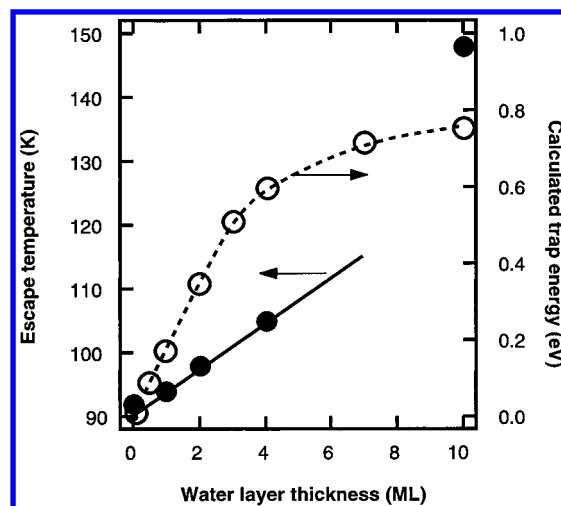


Figure 5. Temperature at which the ions escape the water layer between two 83 ML 3MP layer plotted versus water film thickness (full circles). The temperature is taken from Figure 2, at the dashed line level. Also shown is the predicted well depth versus water thickness (open circles) from calculations in Figure 6.

is shown in Figure 5, on the basis of the temperature at which the curves cross the dashed line in Figure 2. The 10 ML case is ambiguous, as some ion motion is clearly due to loss of solvent rather than ion diffusion/drift: the top 3MP layer begins to desorb just below 130 K, and all the 3MP is gone by 150 K with ion motion occurring over this whole range. For the 10 ML case there are other possibilities for structural changes (discussed later). The delay of the ion motion by the aqueous phase is too large to be attributed to the increase of the ion size that would increase the media’s viscous drag on the ions. A solvation energy trap can account for the large temperature shifts.

We can estimate the solvation energy using a modified Born model.¹⁸ The water and the solvent can be represented by continuum films of thicknesses p_w and p_s and dielectric constants ϵ_w and ϵ_s . The ion is at the center of a hollow sphere of radius r_0 . The electrostatic energy of a monovalent ion, employing a radial field approximation used by Conway,¹⁹ is a volume integral

$$U(\bar{r}_{\text{ion}}) = \iiint d^3r (1 - 1/\epsilon(x,y,z)) \frac{q_e^2}{32\pi^2\epsilon_0(\bar{r} - \bar{r}_{\text{ion}})^4} \quad (2)$$

where q_e is the electron charge and \bar{r}_{ion} is the position of the ion, with $|\bar{r} - \bar{r}_{\text{ion}}| \geq r_0$, the radius of the hydrated ion. This function easily integrates for slabs of the dielectric, even when the hollow sphere overlaps them. This is the “Gibbs” energy of the ion at the interface.²⁰ We used the same approach in an analysis of ions at the “oil”/water interface.²¹ This simple potential ignores the bending of the electric field lines toward the higher dielectric material and should be considered as a semiquantitative estimate.²⁰ The computed energies are shown in Figure 6. Also shown are the water slab for the specific case of a 10-bilayer water film and the excluded volume of the ion. We used $\epsilon_w = 200$ and $\epsilon_s = 1.9$. ϵ_w is not precisely known, but it is believed to be about 200 above 150 K.²² Uncertainty in ϵ_w , however, does not noticeably affect our results because it

(16) Iedema, M. J.; Dresser, M. J.; Doering, D. L.; Rowland, J. B.; Hess, W. P.; Tsekouras, A. A.; Cowin, J. P. *J. Phys. Chem. B* **1998**, *102*, 9203.

(17) Wu, K.; Iedema, M. J.; Tsekouras, A. A.; Cowin, J. P. *Nucl. Instrum. Methods Phys. Res., Sect. B* **1999**, *157*, 259.

(18) Born, M. *Z. Phys.* **1920**, *1*, 45.

(19) Conway, B. E. *J. Electroanal. Chem.* **1975**, *65*, 491.

(20) Volkov, A. G.; Deamer, D. W.; Tanelian, D. L.; Markin, V. S. *Prog. Surf. Sci.* **1996**, *53*, 1 (especially section 11).

(21) Wu, K.; Iedema, M. J.; Cowin, J. P. *Science* **1999**, *286*, 2485.

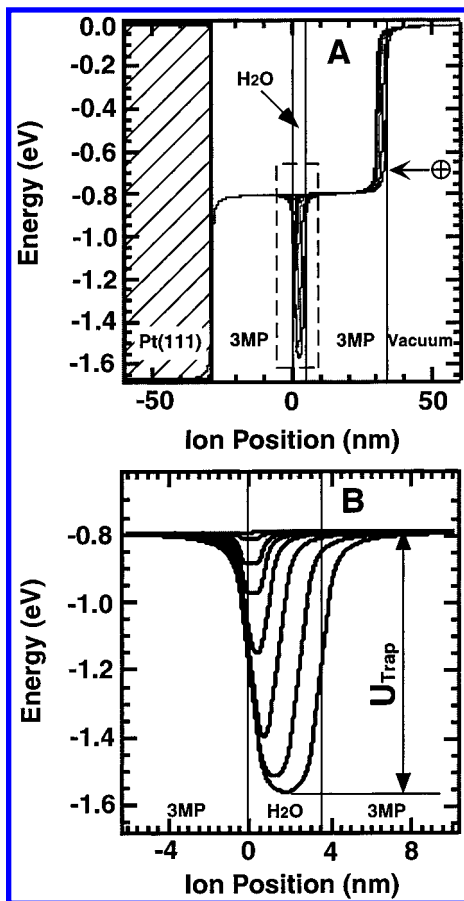


Figure 6. (A) Theoretically calculated potential change that an ion would undergo during its motion from vacuum through the 83 ML 3MP/H₂O/83 ML 3MP sandwich as a function of the water coverage in the middle. The added water coverage for the calculated energy curves, from top to bottom, is 0.0, 0.1, 0.50, 1.0, 2.0, 4.0, 7.0, and 10 ML. Also shown are the slabs for 10 ML of water in the middle of 166 ML 3MP and the excluded volume of the ion. The zero ion position means the ion is at the H₂O/3MP interface closer to the Pt(111) substrate. Positive and negative values on the x-axis indicate that the ion is in the H₂O or top 3MP phases or vacuum and in the bottom 3MP or the Pt(111) metal (hatched area) phases, respectively. (B) Close-up of the area marked by the broken-line rectangle in part A.

appears in the term $(1 - 1/\epsilon_w)$ in eq 2. The only really unknown parameter is r_0 , the hydrated ion shell size. We use 4.3 Å for r_0 (roughly corresponding to the size of the ion with two solvation shells, used in ref 21).

The zero water coverage case (top curve in Figure 6A) shows that at $z=0$ there is a potential that repels the ion away from the vacuum, and the full solvation energy in 3MP is about 0.8 eV. For the 10 ML of water case (bottom curve) the ion is strongly attracted toward the water by the 3MP on either side (see Figure 6B). The trap energy, U_{trap} , is the difference of the potentials in bulk 3MP (at either side of the water slab) and bulk water. This trap energy is plotted versus water thickness (open circles) in Figure 5. The main feature of the ion energetics in the system is that U_{trap} increases with the thickness of the water layer. The trap energy saturates at 0.76 eV (73 kJ/mol) when the water layer is thicker than 20 ML (not shown in Figure 6). It is close to the values calculated by molecular dynamics: 71 kJ/mol for the large ion Cs⁺ moving from bulk water to bulk carbon tetrachloride²³

and 63 kJ/mol for Cl⁻ transferring from bulk water into 1,2-dichloroethane.²⁴

The trap energy explains why the ion motion in the micelles is delayed by the addition of the water layer and why the voltage pause lingers over a wider temperature range with the increase of the water layer thickness. For 10 ML of water, the energy barrier is about 0.75 eV (about 72 kJ/mol), high enough to stop the ion motion until the underlying film begins to desorb (see trace e in Figure 2).

Qualitatively, Figure 5 shows that, from 0 to 4 ML of water, the calculated trap energy is nearly linear with water thickness and further that 10 ML provides a not very much deeper trap than does 4 ML of water. We might expect that the effect of such a trap would be a nearly linear variation in the escape temperature with water coverage, with an offset at low water coverage when the trap becomes kinetically insignificant. Further, we would expect the 10 ML of water data to deviate from a simple linear dependence on water coverage. Looking at Figure 5, we see that the prediction is true (solid line), except for the 10 ML point. The experimental data point for the 10 ML of water layer lies above the simple linear line not below it. We suspect our simple model is perturbed by structural issues and kinetics, as discussed below.

The collective electric field of the ions has a strong effect on the trap energy. We ignore this in our estimation of the trap potentials in Figure 5. It can lower the trap energy by as much as 50%.²¹ But this effect is much less for the last ions to escape, as the collective field they feel is proportional to the density of ions farther from the Pt than they are. So to minimize this effect, we choose as the temperature to plot in Figure 5 that at which the last ions escape the well.

6. Complications and Subtleties. When they reach the water layer, the ions may find more than one potential minimum. The water can act as a rigid barrier to ion passage. Bulk amorphous water is not expected to be liquid at this temperature; 135 K is normally what is reported as its glass temperature (see debate in ref 25). The glass temperature of a 1–10 ML film could be much lower than that for the bulk (as in various polymer glasses²⁶). Now one might conclude that hydronium ions need not disrupt the ice film, as they can exchange a proton with the water film and the proton can tunnel from water to water freely; this is the famous “Grotthuss mechanism”.²⁷ However, experimental and theoretical evidence has mounted to show that this tunneling mechanism is not effective for long range transport in water–ice at these low temperatures, likely both due to self-trapping in a polarization minimum and due to some kinetic barriers for water rearrangements.²⁸ Soft-landing ion studies have never seen that hydronium ions move in amorphous water films of 50 ML and thicker up to 150 K²⁵ or in thicker crystalline ice films up to 190 K.²⁸ Nonetheless, it seems that they can penetrate the thinner films in this micelle-like film study and that there may be kinetic barriers in addition to the potential well trap involved. We suspect that the strong $1/r^2$ fields near the ions are strong enough to overcome any water-film “rigidity”.

Figure 4 shows an interesting energetic phenomenon. On the basis of the Born model, the energetics of 3MP/

(24) Benjamin, I. *Science* **1993**, *261*, 1558.

(25) Wu, K.; Tsekouras, A. A.; Iedema, M. J.; Cowin, J. P. *Phys. Chem. Chem. Phys.*, submitted.

(26) Forrest, J. A.; Dalnoki-Veress, K.; Stevens, J. R.; Dutcher, J. R. *Phys. Rev. Lett.* **1996**, *77*, 2002.

(27) von Grotthuss, C. J. D. *Ann. Chim.* **1806**, *LVIII*, 54.

(28) Cowin, J. P.; Tsekouras, A. A.; Iedema, M. J.; Wu, K.; Ellison, G. B. *Nature* **1999**, *398*, 405.

(22) Tsekouras, A. A.; Iedema, M. J.; Cowin, J. P. *Phys. Rev. Lett.* **1998**, *80*, 5798.

(23) Dang, L. X. *J. Phys. Chem.* **1999**, *103*, 8195.

H₂O/3MP and MCH/H₂O/MCH should be very similar because the dielectric constants of both 3MP and MCH are similar, about 1.9.⁷ Therefore, the trap energy created by the same amount of water (4 ML) should be the same. If one modeled the effect of the trap by placing in the middle of a diffusive medium a kinetic well with an escape rate governed by an Arrhenius expression with the activation energy given by the estimated trap depth and a presumed pre-exponential of 10¹³ s⁻¹, similar as was done in ref 21, then the ion escape from the trap for the MCH case should occur at around the same temperature as it does for the 3MP case, 100 K. This means that trap escape should blend in with the ion migration kinetics for MCH, as the latter also occurs at 100 K. We are attempting more accurate modeling of both the potential and the ion diffusion/migration/trapping. One early result is that the escape from the well has an effective pre-exponential proportional to the solvent viscosity, which should explain the shift of the escape temperature for the trap in the MCH case compared to the 3MP case.

In our simple model the water film is supposed to be uniform in thickness. This may not be true for several reasons. First, the deposition of the water can lead to a statistically higher local water concentration. In the absence of diffusion of the water, a region that on the average would contain 100 waters would routinely have a spread over about the square root of 100, or from 90 to 110, and occasionally less or more. This may be smoothed out by diffusion that can occur as the impinging water loses its excess energy (particularly its heat of binding) over probably several picoseconds. Any such diffusion could make matters worse: Water might "ball-up" locally, as it is not as strongly bound to the hydrocarbon film as it is to itself. This would create thicker water regions and perhaps cracks with no water. Any such cracks would still present a potential trap for the ions, as the adjacent dielectric constant is high. Figure 2 shows some experimental evidence for the nonuniformity of the water layer. Below 4 ML of water, no volcanic desorption of 3MP can be observed (cf. the TPD curves, a–d, in Figure 2). Even for 10 ML of water the volcanic desorption is not fully achieved, that is, the peak area of the volcanic desorption being not so large as expected. Full volcanic desorption can only be observed with the water layer thicker than 15–20 ML. It is possible that the intact water films present an insurmountable kinetic barrier and that only cracks allow ion passage.

Diffusion of water could lead to changes in the film morphology, particularly as the thicker water films delay the ion penetration to higher temperatures. For thin water layers where the ions move through the film only a few degrees higher than they would without the water, the much more rapid motion of ions under these fields compared to neutral diffusion likely prevents significant structural changes during the ion motion. However, at 130 K, these solvents are orders of magnitude less viscous than near 90 K, so neutral diffusion will be inhibited only by the unknown barrier to water molecules diffusing laterally along the water/organic film or "evaporating" into the organic film.

Such diffusion at higher temperatures would have some interesting driving forces. An ion in the water film ought to attract mobile water molecules, making the film locally thicker and the trap deeper. The electric field at the water/organic interface directly under the ion is locally higher than anywhere nearby. If a water molecule migrates to this location to lower its energy, this locally decreases the distance between the water film and the Pt substrate, which in turn increases the field even more locally and

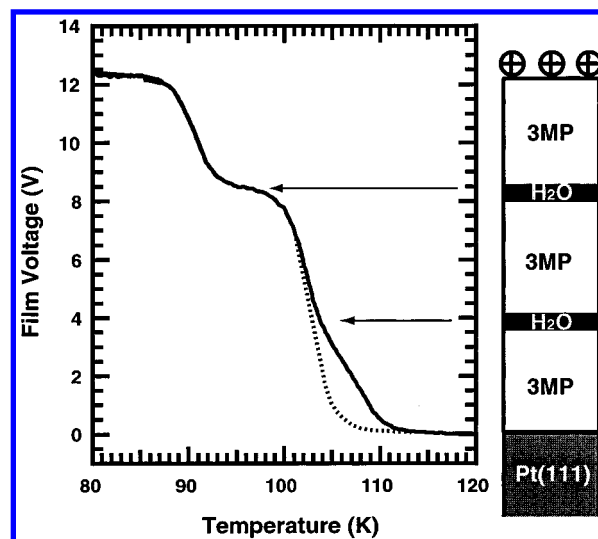


Figure 7. Temperature evolution of the film voltage for a "double-sandwich" film: 83 ML 3MP/4 ML H₂O/83 ML 3MP/4 ML H₂O/83 ML 3MP. The arrows indicate the voltage pauses. The dotted curve is the experimental curve for the film without the lower water layer, namely, 83 ML 3MP/4 ML H₂O/167 ML 3MP. The cartoon on the right side of the figure shows the initial film structure of the "double-sandwich" film (not in proportion).

attracts more water molecules. This could lead to growth of a water whisker. If the supply of water is enough and the organic layer is thin enough, the whisker could reach the Pt surface.

The complications mentioned above are more likely important for thicker water films, where the temperature of ion passage is highest. They provide some interesting opportunities to test these notions. We have not systematically done so yet, as we await completion of more precise modeling. One simple experiment is to make a double sandwich. By putting one water trap, say, at the ²/₃ point in an organic film and the other at the ¹/₃ point, we could delay the ions in the first trap and permit the water at the lower trap to undergo structural rearrangements. The results of such an experiment with two equally thick water layers are shown in Figure 7, for 83 ML 3MP/4 ML H₂O/83 ML 3MP/4 ML H₂O/83 ML 3MP. The voltage shows two pauses, one sharply at ²/₃ and the other vaguely but visibly at ¹/₃ of its initial value. This suggests that the second trap may have become more diffuse while waiting for the ions to arrive. However, since both traps are expected to have the same well depth, the effect of the second trap may be only a shoulder on the escape from the first. Obviously we could use a thinner water layer for the upper trap to separate the detrapping kinetics of the two, or build the micelle structure and preanneal it to various temperatures before adding ions.

Conclusion

In summary, what has been demonstrated in this study is that the soft-landing ion source is an excellent means of probing ion motion into and through micelle-like films and that vapor epitaxy of glassy liquids is a very flexible way to create fairly well-defined obstacle courses to test ideas about ion transport and trapping. This can be done even when the micelles are quite "fragile" (e.g., prone to interdiffusion disruption or nonwetting effects). In MCH/H₂O/MCH and 3MP/H₂O/3MP sandwiches, D₃O⁺ ions first move in normal viscous media (MCH and 3MP) and then are delayed when they meet the aqueous phase in the middle of the micelle-like films. Energetics analysis based

on the modified Born solvation model qualitatively shows that the aqueous phase creates an energy trap to prevent or delay the ion motion. The trap energy increases with the thickness of the aqueous layer. For thicker water films (5–10 monolayers) the temperature of ion detrapping is high enough that structural changes due to diffusion of neutrals and evaporation of organic solvent likely complicate the kinetics. Experimentally, D_3O^+ ions can penetrate thin water layers but are trapped by thick water layers.

Acknowledgment. This work was supported by the U.S. Department of Energy, Basic Energy Sciences, Chemical Sciences Division, and performed at the Wiley Environmental Molecular Sciences Laboratory, a national scientific user facility sponsored by the D.O.E. Office of Biological and Environmental Research. It is located at Pacific Northwest National Laboratory, operated for D.O.E. by Battelle under Contract DE-AC06-76RLO 1830.

LA990852G